A Preclinical Model of CD38-Pretargeted Radioimmunotherapy for Plasma Cell Malignancies

Damian J. Green[1,2], Nural N. Orgun[1], Jon C. Jones[1], Mark D. Hylarides[1], John M. Pagel[1,2], Donald K. Hamlin[3], D.S. Wilbur[3], Yukang Lin[1], Darrell R. Fisher[5], Aimee L. Kenoyer[1], Shani L. Frayo[1], Ajay K. Gopal[1,2], Johnnie J. Orozco[1,2], Theodore A. Gooley[1], Brent L. Wood[1,4], William I. Bensinger[1,2], and Oliver W. Press[1,2]

Abstract

The vast majority of patients with plasma cell neoplasms die of progressive disease despite high response rates to novel agents. Malignant plasma cells are very radiosensitive, but the potential role of radioimmunotherapy (RIT) in the management of plasmacytomas and multiple myeloma has undergone only limited evaluation. Furthermore, CD38 has not been explored as a RIT target despite its uniform high expression on malignant plasma cells. In this report, both conventional RIT (directly radiolabeled antibody) and streptavidin–biotin pretargeted RIT (PRIT) directed against the CD38 antigen were assessed as approaches to deliver radiation doses sufficient for multiple myeloma cell eradication. PRIT demonstrated biodistributions that were markedly superior to conventional RIT. Tumor-to-blood ratios as high as 638:1 were seen 24 hours after PRIT, whereas ratios never exceeded 1:1 with conventional RIT. ^{90}Yttrium absorbed dose estimates demonstrated excellent target-to-normal organ ratios (6:1 for the kidney, lung, liver; 10:1 for the whole body). Objective remissions were observed within 7 days in 100% of the mice treated with doses ranging from 800 to 1,200 μCi of anti-CD38 pretargeted ^{90}Y–DOTA–biotin, including 100% complete remissions (no detectable tumor in treated mice compared with tumors that were 2,982% ± 2,834% of initial tumor volume in control animals) by day 23. Furthermore, 100% of animals bearing NCI-H929 multiple myeloma tumor xenografts treated with 800 μCi of anti-CD38 pretargeted ^{90}Y–DOTA–biotin achieved long-term myeloma-free survival (>70 days) compared with none (0%) of the control animals. *Cancer Res; 74(4); 1179–89. ©2013 AACR.*

Introduction

Bortezomib, lenalidomide, and other novel agents have significantly improved the response rates, progression-free survival, and overall survival for patients with multiple myeloma in recent years (1, 2). Despite these advances, multiple myeloma remains incurable. With currently available therapies, the 77,000 patients with multiple myeloma living in the United States will almost universally relapse and die from progressive disease. Myeloma recurrence is presumably a function of malignant plasma cell clones, and possibly precursor stem cells (3, 4), that evade or develop resistance to available therapies. The efficacy of radioimmunotherapy (RIT) in the treatment of hematologic malignancies is well established (5–7). RIT selectively delivers radiation to target cells at multifocal disease sites and facilitates escalation to radiation doses not achievable through external beam therapy. The radiosensitivity of malignant plasma cells outside of the bone marrow has been well documented in clinical settings. Local recurrence of solitary extramedullary plasmacytomas occurs in less than 10% of cases after external beam radiation alone (8). Radiotherapy is also effective as a palliative measure in patients experiencing pain or other sequelae resulting from multiple myeloma–induced osteolysis. Steep dose–response relationships have been demonstrated for most hematologic malignancies, and the impact of radiation dose escalation may be of particular importance in the case of multiple myeloma (9).

A limited number of radionuclide-based therapies have been explored in the treatment of multiple myeloma (10–14). Although each of these radionuclide-based approaches has theoretical promise, none have directly targeted radiation to the CD38 antigen on multiple myeloma cells. The directed delivery of radionuclides to multiple myeloma cells requires an antigen target that is specific, stable, and uniformly expressed at high density. CD38 is a 45-kDa stable transmembrane glycoprotein receptor expressed at a high epitope density on 95% to 100% of malignant plasma cells (15, 16). The CD38 antigen is expressed on activated T cells, monocytes, and NK (natural killer) cells at relatively low levels when compared with plasma cells. Reports describing CD38 expression on cells that are not of hematopoietic origin have been inconsistent. Nonquantitative approaches have suggested that CD38 may be

Authors' Affiliations: [1]Clinical Research Division, Fred Hutchinson Cancer Research Center; Departments of [2]Medicine, [3]Radiation Oncology, and [4]Laboratory Medicine, University of Washington, Seattle; and [5]Dade Moeller Health Group, Richland, Washington

Note: Supplementary data for this article are available at Cancer Research Online (http://cancerres.aacrjournals.org/).

Corresponding Author: Damian J. Green, Clinical Research Division, Fred Hutchinson Cancer Research Center, 1100 Fairview Avenue N., D3-190, Seattle, WA 98109. Phone: 206-667-5398; Fax: 206-667-1874; E-mail: dgreen@fhcrc.org

doi: 10.1158/0008-5472.CAN-13-1589

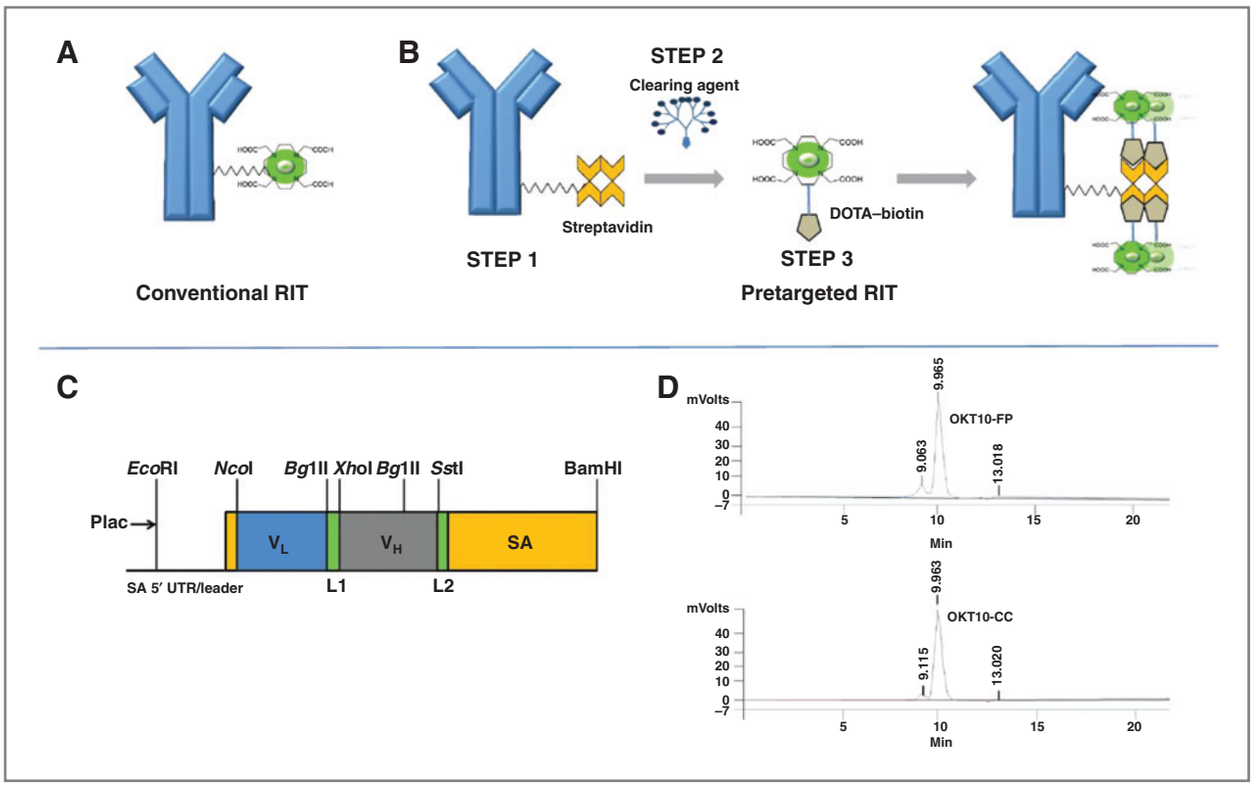

Figure 1. Components for PRIT. Schema depicting one-step conventional RIT (A) and multistep PRIT (B). PRIT involves infusion of the Ab-SA construct (step 1), followed by injection of a synthetic N-acetylgalactosamine–containing clearing agent (step 2) designed to facilitate hepatic clearance of excess Ab-SA from the bloodstream, and then infusion of the radiolabeled small molecule DOTA–biotin (Step 3). C, schematic diagram of OKT10 scFv-SA fusion gene. D, size-exclusion HPLC performed on OKT10-FP and OKT10-CC anti-CD38 streptavidin constructs demonstrate a retention time of 9.965 and 9.963 minutes, respectively. A small amount of aggregate is present.

expressed in pancreatic, lung, brain, and even skeletal muscle (17); however, recent gene expression profiling of human tissues demonstrate that CD38 mRNA is largely restricted to cells of hematopoietic origin with minimal expression in nonhematopoietic derived tissue limited to the thymus and prostate (18).

Unconjugated anti-CD38 monoclonal antibodies (mAb) have induced myeloma cell killing both in culture and in xenograft mouse models (19, 20). CD38 mAbs have reportedly been well tolerated in a small number of patients (21), and a phase I/II clinical trial with the anti-CD38 mAb daratumumab is currently accruing patients with relapsed or refractory multiple myeloma. CD38 mAbs linked to cytotoxic agents have also demonstrated therapeutic activity in myeloma models (22, 23).

Although conventional one-step RIT with directly conjugated radiolabeled antibodies (Fig. 1A) is effective at achieving disease control, disease eradication is thought to be limited by relatively low tumor-to-normal organ ratios of absorbed radioactivity (e.g., 1.5:1 for tumor-to-lung using ^{131}I-anti-CD20; ref. 6). Multistep pretargeting methods can optimize delivery of the therapeutic radionuclide to tumor targets, while limiting normal organs from radiation exposure. Several approaches to pretargeting have been described (24–26). One method uses an antibody–streptavidin (Ab-SA) construct, followed by administration of a small molecule, radio–DOTA–biotin. In the first step, the tumor-reactive Ab-SA localizes to tumor sites without subjecting the rest of the body to nonspecific irradiation. After maximal accumulation of Ab-SA in the tumor, a small molecular weight radioactive moiety (radio–DOTA–biotin) possessing a high affinity for the Ab-SA bound to tumor sites is administered as a second step. Because of its small size, the second-step reagent penetrates the tumors rapidly where it binds tightly to the pretargeted Ab-SA (Fig. 1B). Unbound radio–DOTA–biotin molecules are cleared from the blood and excreted in the urine within minutes. This rapid clearance of the second-step reagent limits the time during which normal tissues are exposed to nonspecific radiation. Dissociating the slow target antigen-binding distribution phase from the radionuclide delivery phase generates more favorable target-to-normal organ ratios. As a further refinement, a clearing agent can be injected shortly before the radiolabeled small molecule to remove unbound Ab-SA from the bloodstream and prevent it from complexing with the radiolabeled small molecule in the circulation (26, 27).

This report describes a new approach to the treatment of multiple myeloma. Anti-CD38 pretargeted RIT (PRIT) demonstrates superior biodistributions when compared with directly labeled conventional anti-CD38 antibody RIT and clear evidence of therapeutic efficacy, which provides a compelling rationale for further study.

Materials and Methods

Cell lines

The human multiple myeloma cell lines NCI-H929 and L363 were a gift from David Maloney [obtained from American Type Culture Collection (ATCC)]. The human Ramos B-cell lymphoma and human RPMI 8226 multiple myeloma cell lines were also obtained from ATCC. The MM1R cell line was a gift from Steven Rosen (Northwestern University, Chicago, IL) and was generated in his laboratory. Cells were grown in RPMI-1640 supplemented with 10% FBS, 50 U/mL penicillin G and 50 μg/mL streptomycin sulfate. Following two passages, cells were frozen and stored in liquid nitrogen for future use. For all studies, a fresh vial of frozen cells was thawed and grown in culture for 7 to 21 days.

Antibodies, antibody conjugates, fusion proteins, and pretargeted reagents

The OKT10 hybridoma expressing murine IgG_1 anti-CD38 Ab and nonspecific IgG_1 control Ab, BHV1 (specific for bovine herpes virus 1), were obtained from ATCC. The OKT10-Ab and BHV1-Ab were produced from ascites in pristine-primed mice purified by HiTrap Protein G HP 5 mL column chromatography. DOTA-Ab reagents were generated as described previously (27). Each Ab-SA was also conjugated to streptavidin (SA) to form covalent synthetic chemical conjugates using previously described methods (27). The CC49 $scFv_4$SA-FP (fusion protein), which recognizes the TAG-72 antigen on human adenocarcinomas, was a gift from NeoRx. Expression, purification, and characterization of CC49-FP have been previously described (28, 29). To produce OKT10-CC, intact OKT10 IgG_1 anti-CD38 mAb was derivatized with either a DOTA (1,4,7,10-tetraazacyclododecane-1,4,7,10-tetraacetic acid) chelate (27, 30) or streptavidin using the heterobifunctional crosslinker SMCC, using methods previously described (27). Iminobiotin and cation exchange chromatography led to purities of >93%. The chemical conjugate (CC) harbors approximately one streptavidin molecule conjugated to each OKT10 molecule as assessed by SDS-PAGE and size-exclusion high-performance liquid chromatography (HPLC; Fig. 1D). OKT10-FP was generated through cloning Fv regions from the OKT10 anti-CD38 hybridoma that were fused to the full-length genomic streptavidin gene of *Streptomyces avidinii*, and the resultant fusion genes (Fig. 1C) expressed as soluble tetramers (174 kDa) in the periplasmic space of *E. coli* (FP construction detailed in Supplementary Methods; ref. 29). Lineweaver–Burke and Scatchard cell binding assays confirmed that both OKT10-CC and OKT10-FP retain the full immunoreactivity and avidity of the parent OKT10-Ab; binding specificity was confirmed by blocking with excess intact unconjugated mAb (Fig. 2A and B). The biotin-binding capacity of the chemical conjugate and fusion protein was similar to recombinant streptavidin by the HABA (4′-hydroxyazobenzene-2-carboxylic acid) assay (not shown).

Radiolabeling

^{90}Yttrium (^{90}Y) and ^{111}Indium (^{111}In; PerkinElmer) radiolabeling of intact DOTA-Ab for conventional RIT and DOTA–biotin for pretargeted RIT was conducted as described previously (27, 30). Radiochemical purity was generally greater than 95% as determined by iTLC and avidin bead assay. DOTA–biotin was synthesized as described in ref. 27.

Trichloroacetic acid precipitation

The amounts of intact and degraded radiolabeled antibody in culture supernatants were estimated by trichloroacetic acid (TCA) precipitation as previously described (Supplementary Methods).

Competitive cell binding assay

L363 cells (0.5×10^6 cells per sample) were plated in a 96-well plate. Serial concentrations of either OKT10-Ab, OKT10 synthetic chemical conjugate (OKT10-CC), OKT10$scFv_4$ fusion protein (OKT10-FP), or isotype control, were added to each well followed by OKT10-APC [0.1 μg, Alexa Fluor 647 Protein Labeling Kit from Molecular Probes (Invitrogen)]. The cells were incubated at 4°C for 45 minutes, washed, and fluorescence intensity was measured on a flow cytometer (Becton Dickinson).

In vitro binding characterization

The CD38 binding ability of OKT10 was assessed using Ramos targeted cells. Cells (0.1×10^6 per sample) were incubated with 30 μL of 10 μg/mL 1F5-Ab (positive control), OKT10-Ab, and BHV1-Ab (nonbinding isotype control) for 30

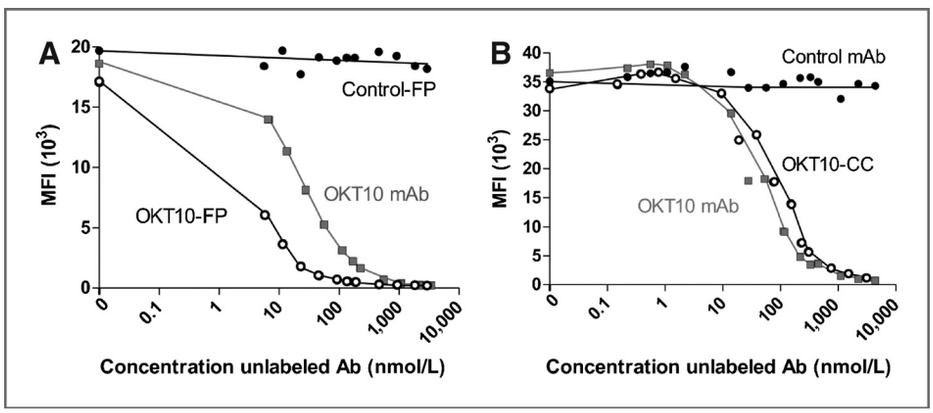

Figure 2. Binding of anti-CD38 antibody constructs to CD38 on malignant plasma cells. Competitive binding assays demonstrate blocking of Alexa-647–conjugated OKT10 mAb binding to CD38-expressing L363 multiple myeloma cells with escalating concentrations of unlabeled OKT10-FP (A) or OKT10-CC (B). No blocking is observed with escalating concentrations of nonbinding control Ab constructs.

minutes at 4°C. Cells were washed and incubated with 25 μL of 1:64 goat anti-mouse IgG (immunoglobulin G; Fab specific) fluorescein isothiocyanate conjugate (Sigma-Aldrich) in PBS. Cells were washed and fluorescence intensity was measured on a FACSCanto I flow cytometer (Becton Dickinson). Binding ability of OKT10 to L363 targeted cells was assessed using OKT10-APC.

Cell binding assay

Anti-CD38 (OKT10-FP/OKT10-CC; 20 μg/mL) or nonbinding control (CC49-FP/BHV1-CC; 20 μg/mL) were added to 1×10^6 cells pelleted in 96-well round-bottomed plates on ice. Pellets were resuspended in the antibody solution, incubated at 4°C for 1 hour, washed, and resuspended in 200 μL Dulbecco's Modified Eagle Medium (DMEM) for 24 hours and stored at 4°C or 37°C. Cells were pelleted and then resuspended in 25 μL of ^{111}In–DOTA–biotin (100 ng/mL), incubated at 4°C for 1 hour, washed twice, and activity was measured on a γ counter.

Mouse RIT and PRIT studies

Female athymic nude-*Foxn1*^{nu} mice, ages 5 to 6 weeks, were purchased from Harlan Sprague-Dawley. NCI-H929 and L363 cells (1×10^7) were injected subcutaneously into the right flank 9 to 11 days before study start dates. Mice bearing palpable plasmacytoma xenografts measuring 100 mm^3 ± 10% were selected for the studies and randomly assigned to experimental groups. Multiple myeloma tumor–bearing mice were placed on a biotin-free diet for 5 days and injected with either 1.4 nmol of anti-CD38 OKT10–DOTA Ab or control BHV1–DOTA Ab, each directly labeled with ^{111}In, or 1.4 nmol of anti-CD38 OKT10 Ab-SA (OKT10-CC or OKT10-FP) or control Ab-SA (BHV1-CC or CC49-scFv$_4$SA-FP), followed 22 hours later by 5.8 nmol (50 μg) clearing agent and 2 hours later by 1.2 nmol (1 μg) of ^{111}In–DOTA–biotin for biodistributions or ^{90}Y–DOTA–biotin labeled with 400 μCi (14.9 MBq), 800 μCi (29.6 MBq), or 1,200 μCi (44.4 MBq) ^{90}Y for therapy studies. Mice were monitored three times weekly for general appearance, tumor volume measurements, and body weight. Mice were injected with anti-asialoGM1 antiserum (200 μL; Wako Chemicals USA, Inc.) 9 and 5 days before the injection of Ab-SA to abrogate NK cell activity and prevent spontaneous tumor regressions. Mice were euthanized when tumors reached a maximum bidirectional measurement of ≥20 × 20 mm, when tumor ulceration occurred, or when mice lost >30% of baseline body weight, as required by the institutional animal care guidelines.

Blood clearance studies

Blood clearance studies were conducted according to the double-label method of Pressman (31, 32). ^{131}Iodine (^{131}I)-OKT10-CC (1.4 nmol) and ^{125}Iodine (^{125}I)-OKT10-FP (1.4 nmol) were coinjected into mice via the tail vein (intravenously). NAGB (N-acetyl-galactosamine-biotin) clearing agent (5.8 nmol) was injected 24 hours later. Venous sampling was conducted via the retro-orbital plexus at serial time points. ^{125}I and ^{131}I were counted on a γ counter, and the percent injected dose per gram (%ID/g) of blood for each radionuclide was calculated. Counts were corrected for ^{131}I crossover into the ^{125}I channel. Counts were also corrected for radioactive decay using an aliquot of the injectate.

Dosimetry

Absorbed radiation doses to organs were calculated for ^{90}Y using β kernel methods for localized β dosimetry expressly developed for accurately calculating the radiation doses to small organs and tissues of the mouse (33, 34). These methods account for energy losses by source and take into account the organ self-dose specific absorbed fractions and the β-particle cross-organ dose contributions. Femoral bone marrow doses were determined using a model that incorporates Monte Carlo calculations of the energy-absorbed fractions in the marrow shafts (35). This model also accounts for the contributions of ^{90}Y on bone surfaces, if any, that may contribute to bone marrow dose.

Statistical analysis

Differences in multiple myeloma tumor xenograft volumes were compared by computing the means and SDs of each treatment group and using the Student *t* test to determine statistical significance. For relatively large differences in tumor volume, 8 to 10 mice per group were projected to provide adequate power to detect statistically significant differences. Only the detection of large differences between treatment groups was considered to be of clinical interest.

Results

OKT10 anti-CD38 reagents are cell-surface stable and enable excellent pretargeting

Experiments assessing the binding and internalization of ^{90}Y-labeled OKT10-Ab and fusion protein were performed using four multiple myeloma cell lines (L363, NCI-H929, RPMI-8226, and MM1R), a CD38-expressing non-Hodgkin lymphoma (NHL) line (Ramos), and four multiple myeloma patient biopsy samples. These studies evaluated the degree of internalization, cell-surface retention, passive dissociation ("shedding"), intracellular metabolism, and exocytosis of ^{90}Y-labeled metabolites, using flow cytometric, cell binding, and "acid-wash" methods as previously published for other targets (36, 37). Only a minority (9% ± 3%; Supplementary Fig. S1) of CD38-targeted Ab or fusion protein was internalized by L363 multiple myeloma tumor cells after 24 hours (the time interval between the two reagents in PRIT). After 24 hours, approximately 60% of initially bound OKT10-Ab remained on the cell surface, whereas 30% to 40% dissociated passively from the cell surface into the culture medium. A TCA precipitation assay was used to demonstrate that the radioactivity released into the culture medium reflected passive "shedding" of intact Ab rather than exocytosis of ^{90}Y-labeled small molecular weight fragments from cells (detailed in Supplementary Materials). To demonstrate effective PRIT targeting of ^{90}Y–DOTA–biotin, multiple myeloma cells were labeled with Ab-SA, washed, and incubated either at 4°C, a temperature that completely inhibits endocytosis, or at 37°C. After 24 hours of incubation, ^{90}Y–DOTA–biotin was added and the amount of radioactivity targeted to multiple myeloma cells was measured. The difference in cell-associated radioactivity was minor, indicating that the magnitude of

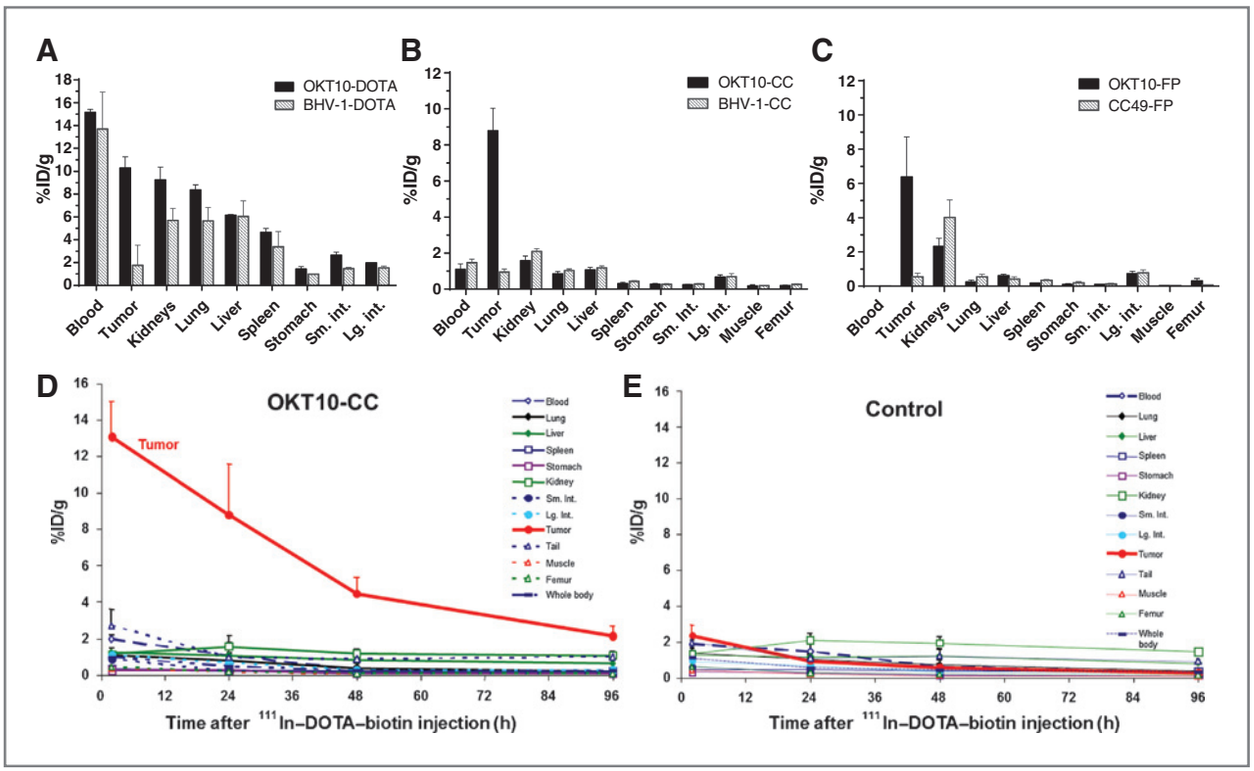

Figure 3. Biodistributions of radioactivity in athymic nude-*Foxn1*^{nu} mice ($n = 5$ per group) bearing CD38$^+$ multiple myeloma xenograft tumors (1×10^7 cells injected into the left flank). Blood, tumor, and normal organ specimens were obtained 24 hours after ^{111}In–OKT10–DOTA or ^{111}In–BHV1–DOTA (control; A), ^{111}In–DOTA–biotin pretargeted by OKT10-CC or BHV1-CC (control CC; B), ^{111}In-DOTA–biotin pretargeted by OKT10-FP or CC49-FP (control fusion protein; C). In PRIT animal studies (B and C), NAGB-clearing agent (5.8 nmol) was administered 2 hours before the ^{111}In–DOTA–biotin (1.2 nmol). Comprehensive tissue biodistributions of radioactivity obtained at sequential time-points 2, 24, 48, and 96 hours following ^{111}In–DOTA–biotin are shown for the mice from the OKT10-CC (D) and BHV1-CC (E) PRIT groups.

endocytosis of the first-step reagent in 24 hours was not sufficient to prevent effective targeting of the second-step reagent (^{90}Y–DOTA–biotin). Concordant results were seen for three other cell lines and the patient samples tested. These conclusions also pertain *in vivo* since favorable *in vivo* targeting of ^{111}In–DOTA–biotin to xenografts is observed (Fig. 3B–E).

Comparative biodistributions of radioactivity demonstrate OKT10 PRIT improves the therapeutic index

Blood, tumor, and nonspecific organ uptake of one-step directly radiolabeled (conventional) OKT10 (OKT10–DOTA) was compared with multistep PRIT in six biodistribution experiments involving athymic nude mice bearing subcutaneous CD38$^+$ human myeloma tumor xenografts (NCI-H929 and L363). Studies were designed to evaluate the relative merits of two distinct pretargeting constructs, OKT10-CC and OKT10-FP (administered at equimolar concentrations). Sixteen groups of 5 mice each were injected with 1.4 nmol of OKT10–DOTA, OKT10-FP, or OKT10-CC (including matched antibody isotype or fusion protein–matched controls). The PRIT reagents (OKT10-FP or OKT10-CC) were followed, 18 to 22 hours later, by 5.8 nmol clearing agent and 2 hours thereafter by 1.2 nmol ^{111}In–DOTA–biotin (1 μg). Groups of animals were euthanized at 2, 24, 48, and 96 hours after injection of the radioactivity. Tumors excised from mice pretargeted with OKT10-CC contained 8.8% ± 2.8% of the injected dose of ^{111}In–DOTA–biotin per gram (%ID/g) after 24 hours compared with 0.9 ± 0.4 %ID/g after 24 hours in tumors excised from control mice pretargeted with a control Ab-SA chemical conjugate (BHV1-CC; all values are mean ± SD; Fig. 3B). The 24-hour tumor-to-normal organ ratios of absorbed radioactivity were 10:1; 8:1; and 6:1, respectively for lung, liver, and kidney in mice pretargeted with OKT10-CC; compared with <1:1 for the lung, liver, and kidney in control mice pretargeted with BHV1-CC.

Tumors excised from mice pretargeted with OKT10-FP demonstrated uptakes of radioactivity in tumor sites (6.4 %ID/g ± 2.3% after 24 hours) that were similar to those observed with the chemical conjugate, whereas minimal tumor uptakes were seen in the controls treated with CC49-FP (0.55 %ID/g ± 0.21% after 24 hours; all values are mean ± SD; Fig. 3C). Tumor-to-organ ratios of absorbed radioactivity with OKT10-FP PRIT were 27:1; 10:1, and 3:1, respectively, for lung, liver, and kidney at the 24-hour time point compared with ≤1:1 for the same organs in control mice pretargeted with the negative control CC49-FP. The minimal tumor uptake of radiobiotin detected in both the CC49-FP and BHV1-CC control groups demonstrates the specificity of targeting with OKT10-FP and OKT10-CC (Fig. 3B and C).

Although levels of radioactivity in tumor xenografts measured 24 hours after administration of the radioactive species were similar in the OKT10-FP, OKT10-CC, and OKT10–DOTA–treated mice (6.4% ± 2.3%, 8.8 ± 2.8 %ID/g, and 9.4% ± 2.2%, respectively), PRIT (OKT10-CC and OKT10-FP) led to biodistributions of radioactivity that were far superior to the conventional (OKT10–DOTA) approach (Fig. 3A–E). At 24 hours following injection of the radiolabeled species, the tumor-to-blood ratio for the conventional RIT was <1:1, whereas for the OKT10-FP and OKT10-CC, ratios were 638:1 and 9:1, respectively, confirming the capacity for PRIT to circumvent the tumor-to-normal organ distribution limitations seen with conventional one-step RIT (38, 39).

Excellent target specificity was demonstrated for both PRIT constructs. Although tumor-to-blood ratios were most dramatic with the fusion protein, this finding seems to be a consequence of very rapid circulatory clearance of the fusion protein (see blood clearance studies below) and did not lead to superior overall biodistributions. For both constructs, the kidney represented the normal organ with the largest nonspecific radiation uptake. Tumor-to-kidney ratios were 6:1 and 3:1 for the chemical conjugate and fusion protein, respectively, 24 hours after the ^{111}In–DOTA–biotin infusion. Thus, the kidney was identified as the organ likely to define dose-limiting toxicity in high-dose therapy settings, and the findings supported an overall advantage for OKT10-CC pretargeting.

Blood clearance studies favor OKT10-CC

Optimal tumor target accretion in PRIT models requires a sustained concentration of the first-step streptavidin reagent in the bloodstream during the biodistribution phase of the treatment algorithm, followed by rapid blood clearance after administration of biotinylated polymeric N-acetyl-galactosamine clearing agent. The rapid clearance of OKT10-CC or fusion protein complexed with clearing agent is mediated by asialoglycoprotein receptors in the liver (26). Detailed blood clearance studies conducted in athymic mice both when administered separately and coinjected (32) with both ^{131}Iodine (^{131}I)-OKT10-CC and ^{125}Iodine (^{125}I)-OKT10-FP at equimolar concentrations revealed that 16% of the OKT10-CC remained in the circulation 24 hours after injection, compared with only 1.4% of the OKT10-FP (not shown).

Synthetic clearing agent reproducibly removed >85% of circulating OKT10-CC or OKT10-FP from the bloodstream within 60 minutes of administration in five blood clearance studies. In a representative experiment, clearing agent (5.8 nmol) was injected 24 hours after ^{131}I-OKT10-CC (300 μg) into 5 athymic nude mice (intravenously). Retro-orbital venous sampling was conducted at serial time points up to 24 hours and ^{131}I was counted on a γ counter. After clearing agent administration, the concentration of ^{131}I-OKT10-CC dropped from 22.8 ± 3.1 %ID/g of blood to 3.2 ± 0.3 %ID/g 60 minutes later (all values are mean ± SD; Fig. 4). Consistent with prior studies (27), reequilibration with conjugate in the extravascular space caused a slight rebound rise of the ^{131}I-OKT10-CC during the subsequent 2 hours (Fig. 4).

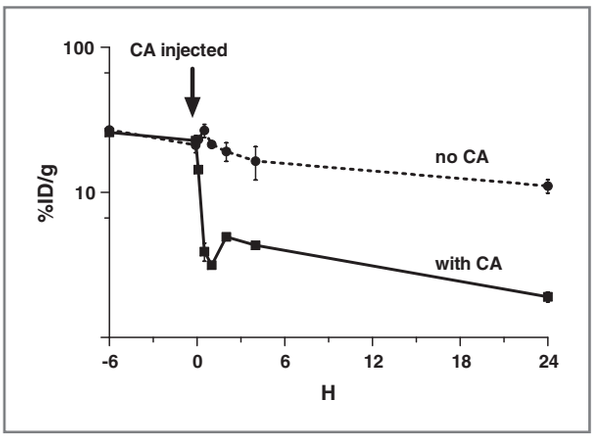

Figure 4. Effects of biotinylated N-acetyl galactosamine clearing agent on circulating OKT10-CC. Clearing agent (CA; 5.8 nmol) was injected 24 hours after ^{131}I-OKT10-CC (1.4 nmol) into 5 athymic nude mice (intravenously). Five control mice received ^{131}I-OKT10-CC (1.4 nmol) and no clearing agent. Retro-orbital venous sampling was conducted at serial time points up to 24 hours.

Organ dosimetry

A detailed organ dosimetry analysis was performed to calculate ^{90}Y absorbed dose estimates after OKT10-CC pretargeting (Fig. 5). Radiation-absorbed doses to tumors, whole body, and nine normal tissues were determined on the basis of integrating the areas under time–activity curves constructed by plotting the concentration of ^{111}In–DOTA–biotin in tissues after various intervals of time (33). The dosimetry method used accounted for organ self-dose absorbed fractions as well as β-particle cross-organ dose contributions (33). The ^{90}Y absorbed dose estimates (Gy) per millicurie administered, calculated from the ^{111}In tracer, generated tumor-to-normal organ ratios of 6:1 for the kidney, lung, and liver, 15:1 for the spleen, and 10:1 for the whole body.

Therapy studies

^{90}Y–DOTA–biotin pretargeted to CD38 eradicates plasmacytomas in vivo. Therapy studies were performed in athymic mice (n = 8–10 per group) bearing subcutaneous xenografts of either L363 or NCI-H929 malignant plasma cells, producing tumors similar to human plasmacytomas. Reagent concentrations and time-points for administration of OKT10-CC, BHV1-CC, and clearing agent were identical to those reported for the biodistribution studies.

^{90}Y–DOTA–biotin (2 μg) was labeled with 400, 800, or 1,200 μCi per mouse in three OKT10-CC groups and three control groups (untreated control; 800 or 1,200 μCi ^{90}Y–DOTA–biotin after BHV1-CC). All L363 tumor xenograft mice in the untreated control and BHV1-CC control groups experienced exponential multiple myeloma tumor growth and 78% of the untreated control animals required euthanasia within 17 days (Fig. 6A). After 22 days, 100% of the 800 μCi and 89% of 1,200 μCi BHV1-CC control groups had required euthanasia due to progressive tumor growth. All mice pretargeted with OKT10-CC followed by ^{90}Y–DOTA–biotin demonstrated tumor shrinkage by day 6 at all dose

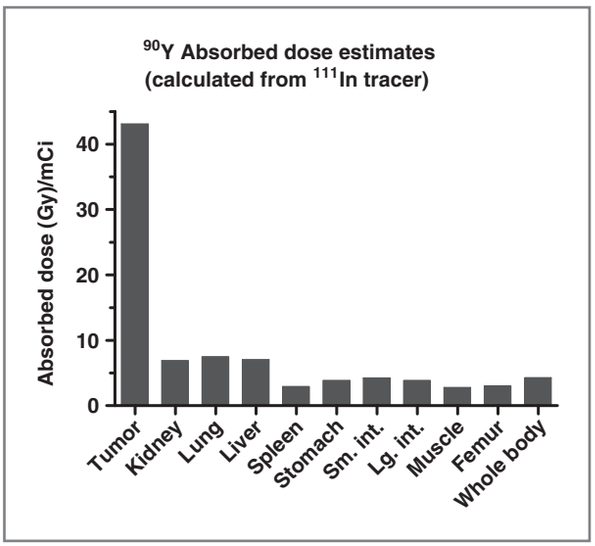

Figure 5. ^{90}Y absorbed dose estimates (Gy/mCi) from an ^{111}In–DOTA–biotin tracer. Radiation absorbed doses to tumor, whole body, and normal tissues are estimated by integrating the areas under time–activity curves constructed by plotting the concentration of ^{111}In–DOTA–biotin (after OKT10-CC pretargeting) measured in tissues by γ counting at 2, 24, 48, and 96 hours (33).

levels (Fig. 6A). After 20 days, 90% of the OKT10-CC–treated animals in the 400, 800, and 1,200 μCi groups remained alive. One animal treated with 1,200 μCi was euthanized on day 10 due to weight loss (as required by the institutional animal care guidelines); however the other 9 animals from that group were healthy, weighing 106% ± 9% (SD) of initial body weight on day 17 (Supplementary Fig. S2). Objective remissions were observed within 6 days in 100% of the mice treated with OKT10-CC, followed by 1,200 μCi of ^{90}Y–DOTA–biotin, including 100% complete remissions (no detectable tumor in OKT10-CC–treated mice compared with tumors that were 5,240% ± 2,495% of initial tumor volume in untreated control animals) by day 17 ($P < 0.0001$, Student t test; Fig. 6A). After 100 days, 70% of the OKT10-CC–treated animals in the 1,200 μCi group, 30% in the 800-μCi group, and 20% in the 400 μCi group remained alive and tumor-free (Fig. 6B). In mice bearing NCI-H929 multiple myeloma xenograft tumors, 800 μCi pretargeted to OKT10-CC was sufficient to eradicate 100% of tumor xenografts within 23 days. At the identical time point, tumors progressed in all BHV1-CC–treated controls receiving 800 μCi. Control tumors were 2,982% ± 2,834% of the initial tumor volume ($P < 0.0001$, Student t test; Fig. 6C). Seventy days after treatment with 800 μCi of anti-CD38 pretargeted ^{90}Y–DOTA–biotin, 100% of animals initially bearing NCI-H929 multiple myeloma tumor xenografts were alive, compared with no mice surviving in the control group (Fig. 6D). Hepatic and renal function was assessed through measurement of serum transaminases, blood urea nitrogen (BUN), and creatinine levels 160 days after the mice received ^{90}Y–DOTA–biotin (800 μCi; $n = 5$). No significant toxicity was observed. The measured serum creatinine was <0.4 mg/dL in all animals, the average BUN, ALT, and AST values were 48 ± 33 mg/dL, 46.8 ± 40 U/L, and 120.4 ± 116.7 U/L, respectively.

Tumor-to-normal organ ratios from the PRIT biodistribution studies described above were markedly superior to conventional RIT and provided the rationale for dose escalation up to 1,200 μCi in PRIT therapy studies. In contrast with the efficacy and tolerability demonstrated with anti-CD38 PRIT, conventionally radiolabeled ^{90}Y–OKT10–DOTA administered as a single step to athymic nude mice ($n = 10$/group) bearing subcutaneous NCI-H929 tumor xenografts was not well tolerated. Within 15 days of infusion, 100% of animals receiving 400 μCi of ^{90}Y–OKT10–DOTA died from complications of radiation toxicity [weight loss, thrombocytopenia (petechiae), and failure to thrive]. On day 8, these animals weighed 79% ± 9% of their initial body weight. When mice were treated with 200 μCi of ^{90}Y–OKT10–DOTA, all tumor xenografts transiently decreased in size, but 6 of 10 animals exhibited tumor progression by day 40 and 1 animal died of radiation toxicity on day 19. All animals in the untreated and ^{90}Y–BHV1–DOTA control groups (200 and 400 μCi) had either died of tumor progression or radiation toxicity (60%), or demonstrated tumor growth by day 40 (not shown).

To assess if any of the observed antitumor activity is attributable to the CD38 mAb in the absence of radiolabeled DOTA–biotin, mice bearing L363 multiple myeloma xenografts ($n = 10$) were treated with OKT10-CC administered as a single agent without subsequent ^{90}Y–DOTA–biotin infusion. These animals treated with OKT10-CC alone demonstrated no tumor response and 100% required euthanasia by day 17 for tumors that were 7,837% ± 3,492% of their initial volume. In contrast, a matched cohort of mice ($n = 10$), treated concurrently with identical doses of OKT10-CC followed by clearing agent and ^{90}Y–DOTA–biotin, (800 μCi) demonstrated complete remissions by day 17 in 100% of animals, and 70% of these animals were alive and tumor free at day 80 (Fig. 7A and B).

Discussion

Plasma cell malignancies, including multiple myeloma, are rarely cured. Despite the higher response rates and longer survival afforded by novel agents (1, 2), the vast majority of patients with plasma cell malignancies die of progressive disease, emphasizing the importance of continuing to investigate new treatment strategies. RIT is a therapeutic modality that is not cross-resistant with chemotherapy or "novel agents" and has been underexplored in this disease.

External beam radiation can cure isolated malignant plasmacytomas and radiotherapy is frequently used to palliate painful multiple myeloma bone lesions. Sustained local disease control and durable symptom relief has been reported for 98% of lesions receiving >10 Gy (40). Furthermore, the poor prognostic implications associated with high-risk bone marrow cytogenetics in active multiple myeloma are not predictive of a decrement in the very high rates of local control and cure after external beam radiotherapy is used to treat solitary extramedullary plasmacytomas with the same cytogenetic derangements (41). This suggests that the unique attributes associated with the targeted delivery of radiation may augur clinical

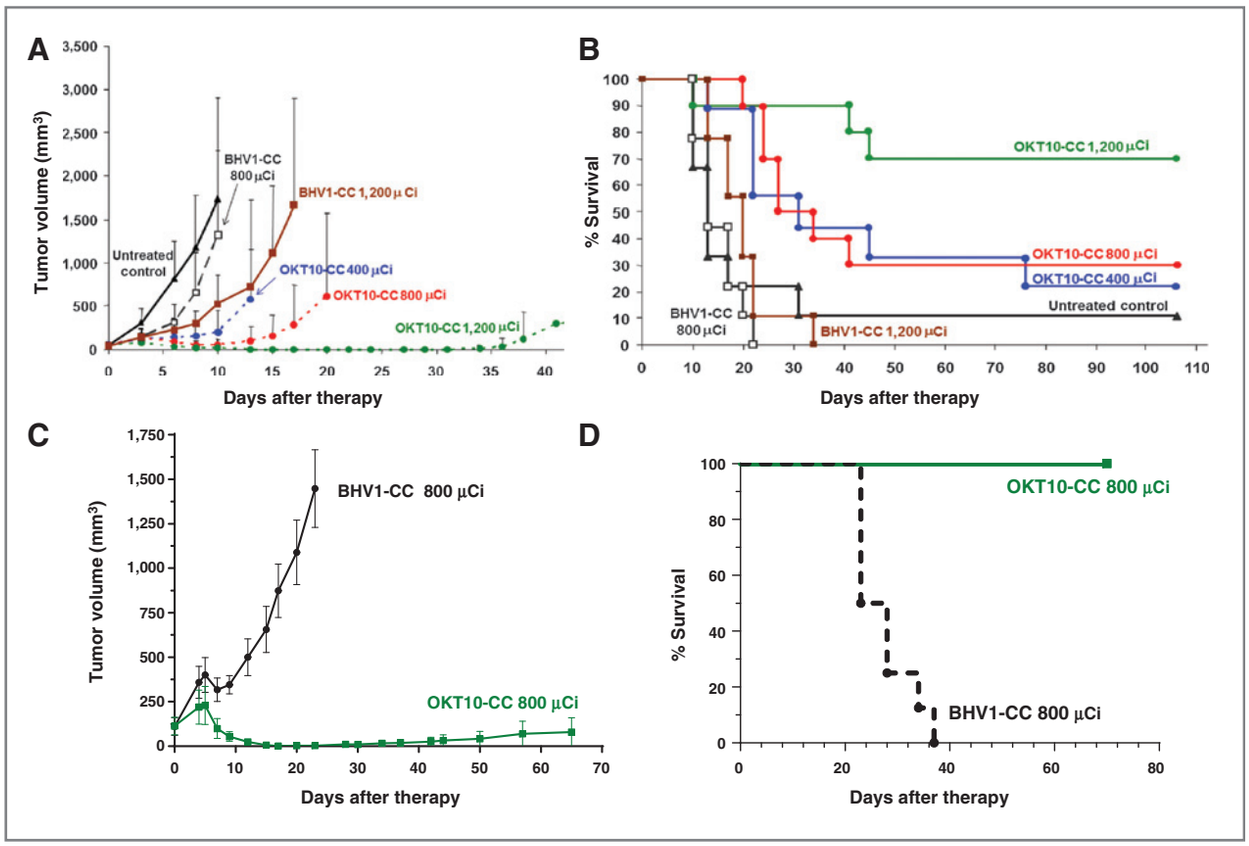

Figure 6. Tumor responses in athymic nude mice ($n = 8$–10 per group) bearing L363 (A and B) or NCI-H929 (C and D) right flank multiple myeloma xenografts. Mice received 1.4 nmol (300 μg) of OKT10-CC or BHV1-CC (control) and clearing agent [5.8 nmol (50 μg)]. Treatment groups received ^{90}Y–DOTA–biotin 24 hours after the OKT10-CC at doses of 400 μCi (14.9 MBq), 800 μCi (29.6 MBq), and 1,200 μCi (44.4MBq); and at doses of 800 μCi and 1,200 μCi for the BHV1-CC control groups. A, mice were monitored three times weekly for tumor volume measurements and were euthanized when tumors were ≥10% of body weight or when ulceration occurred, as mandated by the Institutional Animal Care Committee. Curves are truncated at the time the first animal was euthanized in each group. A dose-dependent regression of multiple myeloma tumor xenografts is demonstrated. B, Kaplan–Meier analysis of cumulative survival of mice bearing L363 multiple myeloma xenografts. C, NCI-H929 treatment groups received 800 μCi (29.6 MBq) of ^{90}Y–DOTA–biotin 24 hours after the OKT10-CC or BHV1-CC (control group). Complete regression of multiple myeloma tumor xenografts in the OKT10-CC group is demonstrated. D, Kaplan–Meier survival analysis of mice bearing NCI-H929 multiple myeloma xenografts.

efficacy even among patients classified as "high risk". When ionizing radiation has been combined with bortezomib, synergistic inhibition of multiple myeloma cell proliferation has been reported (12). It has also been suggested that the efficacy of bortezomib can be improved when combined with skeletally targeted ^{153}samarium lexidronam (42). These findings raise the possibility that anti-CD38 RIT may be enhanced when combined with novel therapies.

Although several plasma cell–associated antigens have been identified, we elected to target CD38 because it has a high density and consistency of expression on clonal plasma cells (15, 16). We demonstrate that the receptor has minimal internalization and is not shed from the plasma cell surface after binding to OKT10. The unmodified CD38 mAb daratumumab, which binds a unique epitope on the antigen receptor, has demonstrated anti-multiple myeloma tumor cell activity both *in vitro* and in mouse xenografts (19); however, perhaps as a consequence of binding a different epitope, OKT10-CC administered as a single agent without radioactivity demonstrates no antitumor effects. The promising results achieved with daratumomab, however, complement our approach targeting CD38 for radionuclide delivery and validate the antigen as a desirable target. Despite the salient favorable attributes enumerated for CD38, no target antigen is perfect and it must be acknowledged that CD38 expression is not limited exclusively to malignant plasma cells. Nevertheless, the expression of CD38 on normal plasma cells and some activated lymphoid cells must be viewed in the context of the successful selection strategies that have resulted in clinically approved RIT therapeutics for other hematologic malignancies, such as ^{131}Iodine-tositumomab (Bexxar) and ^{90}Yttrium-ibritumomab tiuxetan (Zevalin). The efficacy and favorable toxicity profiles of anti-CD20 RIT in B-cell lymphoma have been clearly established despite expression of this antigen on normal B cells (5–7). The CD38 antigen has many attributes parallel to CD20 to support its selection as a viable target for RIT.

Several therapeutic radionuclides might be considered for RIT of multiple myeloma. We selected ^{90}Y as the radioisotope for these studies because it is a pure, high-energy β-emitter that is readily complexed by the DOTA chelate and is commercially

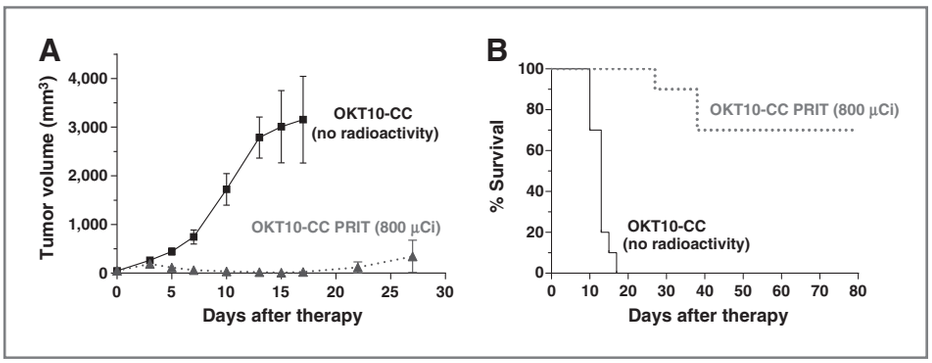

Figure 7. Tumor responses in athymic nude mice ($n = 10$ per group) bearing L363 right flank multiple myeloma xenografts. All mice received 1.4 nmol (300 μg) of OKT10-CC as a single agent (no radioactivity) or followed by clearing agent [5.8 nmol (50 μg)] and ^{90}Y–DOTA–biotin [800 μCi (29.6 MBq)] 24 hours after the OKT10-CC. A, mice were monitored three times weekly for tumor volume measurements and were euthanized when tumors were ≥10% of body weight or when ulceration occurred, as mandated by the Institutional Animal Care Committee. Curves are truncated at the time the first animal was euthanized in each group. Complete regression of multiple myeloma tumor xenografts in the group receiving OKT10-CC followed by 800 μCi (29.6 MBq) is demonstrated. Animals receiving OKT10-CC as a single agent (no radioactivity) demonstrated rapid tumor progression. B, Kaplan–Meier analysis of cumulative survival of mice bearing L363 multiple myeloma xenografts.

available in high specific activity and purity. The long path length of ^{90}Y's β particles permits the delivery of lethal radiation across several cell diameters, resulting in a "crossfire effect" that can eradicate antigen-negative multiple myeloma cells (or multiple myeloma cells that are in the center of a tumor cluster) by lethal radiation emitted from surrounding antibody-binding CD38$^+$ multiple myeloma cells. Furthermore, the current biotin reagents used for PRIT can only accommodate radiometals, not ^{131}I, and attempts to produce effective ^{131}I-labeled biotin have generally been disappointing, reenforcing the selection of ^{90}Y.

In this report, we demonstrate that the ^{90}Y-based anti-CD38 PRIT approach chosen, rapidly and completely eradicates plasmacytoma xenografts with minimal toxicity. This therapeutic efficacy was predicted by anti-CD38 PRIT biodistributions that were markedly superior to those achievable by conventional RIT, as confirmed by radiation dosimetry estimates demonstrating excellent tumor-to-normal organ ratios. Although both anti-CD38-SA constructs were effective, the rapid circulatory clearance of OKT10-FP resulted in a lower area under the curve (AUC) during the distribution phase; and, despite excellent blood-to-tumor ratios of activity, the fusion protein had lower tumor-to-kidney ratios of absorbed activity (3:1) when compared with OKT10-CC PRIT (6:1) after 24 hours. Consistent with prior published reports, biodistribution studies predicted the kidney to be the dose-limiting normal organ (43). The renal biodistribution profile for the chemical conjugate, therefore, provided a rationale for selection of OKT10-CC as the best pretargeting reagent for subsequent therapy studies.

PRIT enables the administration of ^{90}Y doses not attainable using conventional one-step RIT and seems to improve the therapeutic index, enhance efficacy, and diminish toxicity. Removal of excess OKT10-CC from the vascular compartment by clearing agent, combined with rapid urinary excretion of excess ^{90}Y–DOTA–biotin, limited nonspecific radiation exposure to normal organs even at doses of 1,200 μCi (three times the previously defined lethal doses in conventional ^{90}Y labeled RIT; ref. 44). Ninety percent of animals in the highest dose group demonstrated only mild transient weight loss, and regained their normal weight within 15 days (Supplementary Fig. S2), whereas animals receiving either 400 or 800 μCi demonstrated no significant drop in weight. Among the OKT10-CC animals alive and disease free >70 days after therapy, no significant toxicity was detectable.

We elected to initiate preclinical studies of CD38-targeted RIT and PRIT using a plasmacytoma model because traditional radiation dosimetry and biodistribution methods can be most accurately performed using solid tumor nodules, and are much more difficult to apply in a quantitative fashion using marrow–based, disseminated disease. Tumor xenografts are, therefore, the standard for initial RIT validation studies (e.g., CD20 in NHL, CD45 in acute myeloid leukemia; refs. 27, 45–48). In addition, xenograft models have played a vital role in validating the impressive efficacy of proteasome inhibitor therapy in multiple myeloma and we have emulated this initial approach (49).

Despite serving as a well-validated model for the assessment of new RIT targets and multiple myeloma therapeutics in large cohorts of animals, multiple myeloma tumor xenografts do not fully recapitulate the clinical spectrum of the disease (49, 50). The absence of human CD38 antigen expression in murine tissues is an inherent limitation of most xenograft models, and the xenograft model applies most directly to soft tissue plasmacytomas rather than disseminated multiple myeloma. Furthermore, xenografts do not provide a bone-based platform that recapitulates the human marrow microenvironment. To address this concern, we are conducting studies in a SCID-hu multiple myeloma mouse model and have seen preliminary results that are encouraging, but beyond the scope of the current article.

In conclusion, this is the first report of anti-CD38 RIT in multiple myeloma and the first report documenting the efficacy of PRIT in this disease. The complete eradication of multiple myeloma tumor xenografts provides a scientifically compelling rationale for further exploring high-dose anti-CD38

PRIT as conditioning therapy before autologous stem-cell transplant for multiple myeloma. Although xenograft tumors are not ideal, they have been used to accurately predict the value of CD20 and CD45 directed RIT or PRIT in lymphoma and leukemia mouse models, and have been used to establish the value of "novel agents" to treat multiple myeloma despite the same limitations. Ultimately, clinical trials will be necessary to demonstrate safety and evaluate the potential for anti-CD38 PRIT to improve progression-free and long-term survival among patients with multiple myeloma.

Disclosure of Potential Conflicts of Interest

No potential conflicts of interest were disclosed.

Authors' Contributions

Conception and design: D.J. Green, J.C. Jones, J.M. Pagel, D.S. Wilbur, A.K. Gopal, O.W. Press

Development of methodology: D.J. Green, J.C. Jones, M.D. Hylarides, J.M. Pagel, D.K. Hamlin, D.S. Wilbur, Y. Lin, D.R. Fisher, A.K. Gopal, O.W. Press

Acquisition of data (provided animals, acquired and managed patients, provided facilities, etc.): D.J. Green, N.N. Orgun, J.C. Jones, M.D. Hylarides, D.S. Wilbur, D.R. Fisher, S.L. Frayo, J.J. Orozco, B.L. Wood, O.W. Press

Analysis and interpretation of data (e.g., statistical analysis, biostatistics, computational analysis): D.J. Green, N.N. Orgun, J.M. Pagel, D.S. Wilbur, D.R. Fisher, A.K. Gopal, T.A. Gooley, B.L. Wood, W.I. Bensinger, O.W. Press

Writing, review, and/or revision of the manuscript: D.J. Green, J.M. Pagel, D. S. Wilbur, Y. Lin, D.R. Fisher, S.L. Frayo, A.K. Gopal, J.J. Orozco, B.L. Wood, W.I. Bensinger, O.W. Press

Administrative, technical, or material support (i.e., reporting or organizing data, constructing databases): D.J. Green, A.L. Kenoyer

Study supervision: D.J. Green, J.M. Pagel, O.W. Press

Grant Support

This work was supported by grants from the U.S. NIH NCI K08 CA151682 (D.J. Green), NCI R01 CA154897, and NCI R01 CA076287 (O.W. Press), Multiple Myeloma Research Foundation Research Fellow Award (D.J. Green), and The Orin Edson Foundation (D.J. Green and O.W. Press).

The costs of publication of this article were defrayed in part by the payment of page charges. This article must therefore be hereby marked *advertisement* in accordance with 18 U.S.C. Section 1734 solely to indicate this fact.

Received June 3, 2013; revised November 14, 2013; accepted December 2, 2013; published OnlineFirst December 26, 2013.

References

1. Kumar SK, Rajkumar SV, Dispenzieri A, Lacy MQ, Hayman SR, Buadi FK, et al. Improved survival in multiple myeloma and the impact of novel therapies. Blood 2008;111:2516–20.
2. Anderson KC. The 39th David A. Karnofsky Lecture: bench-to-bedside translation of targeted therapies in multiple myeloma. J Clin Oncol 2012;30:445–52.
3. Pilarski LM, Hipperson G, Seeberger K, Pruski E, Coupland RW, Belch AR. Myeloma progenitors in the blood of patients with aggressive or minimal disease: engraftment and self-renewal of primary human myeloma in the bone marrow of NOD SCID mice. Blood 2000;95: 1056–65.
4. Matsui W, Wang Q, Barber JP, Brennan S, Smith BD, Borrello I, et al. Clonogenic multiple myeloma progenitors, stem cell properties, and drug resistance. Cancer Res 2008;68:190–7.
5. Nademanee A, Forman S, Molina A, Fung H, Smith D, Dagis A, et al. A phase 1/2 trial of high-dose yttrium-90-ibritumomab tiuxetan in combination with high-dose etoposide and cyclophosphamide followed by autologous stem cell transplantation in patients with poor-risk or relapsed non-Hodgkin lymphoma. Blood 2005;106: 2896–902.
6. Press OW, Eary JF, Appelbaum FR, Martin PJ, Badger CC, Nelp WB, et al. Radiolabeled-antibody therapy of B-cell lymphoma with autologous bone marrow support. N England J Med 1993;329:1219–24.
7. Kaminski MS, Tuck M, Estes J, Kolstad A, Ross CW, Zasadny K, et al. 131I-tositumomab therapy as initial treatment for follicular lymphoma. N England J Med 2005;352:441–9.
8. Kumar S. Solitary plasmacytoma: is radiation therapy sufficient? Am J Hematol 2008;83:695–6.
9. Gluck S, Van Dyk J, Messner HA. Radiosensitivity of human clonogenic myeloma cells and normal bone marrow precursors: effect of different dose rates and fractionation. Int J Radiat Oncol, Biol, Phys 1994; 28:877–82.
10. Giralt S, Bensinger W, Goodman M, Podoloff D, Eary J, Wendt R, et al. 166Ho-DOTMP plus melphalan followed by peripheral blood stem cell transplantation in patients with multiple myeloma: results of two phase 1/2 trials. Blood 2003;102:2684–91.
11. Rousseau C, Ferrer L, Supiot S, Bardies M, Davodeau F, Faivre-Chauvet A, et al. Dosimetry results suggest feasibility of radioimmunotherapy using anti-CD138 (B-B4) antibody in multiple myeloma patients. Tumour Biol 2012;33:679–88.
12. Goel A, Dispenzieri A, Geyer SM, Greiner S, Peng KW, Russell SJ. Synergistic activity of the proteasome inhibitor PS-341 with non-myeloablative 153-Sm-EDTMP skeletally targeted radiotherapy in an orthotopic model of multiple myeloma. Blood 2006;107:4063–70.
13. Kapoor P, Greipp PT, Morice WG, Vincent Rajkumar S, Witzig TE, Greipp PR. Anti-CD20 monoclonal antibody therapy in multiple myeloma. British J Haematol 2008;141:135–48.
14. Supiot S, Faivre-Chauvet A, Couturier O, Heymann MF, Robillard N, Kraeber-Bodere F, et al. Comparison of the biologic effects of MA5 and B-B4 monoclonal antibody labeled with iodine-131 and bismuth-213 on multiple myeloma. Cancer 2002;94:1202–9.
15. Deaglio S, Aydin S, Vaisitti T, Bergui L, Malavasi F. CD38 at the junction between prognostic marker and therapeutic target. Trends Mol Med 2008;14:210–8.
16. Bataille R, Jego G, Robillard N, Barille-Nion S, Harousseau JL, Moreau P, et al. The phenotype of normal, reactive and malignant plasma cells. Identification of "many and multiple myelomas" and of new targets for myeloma therapy. Haematologica 2006;91:1234–40.
17. Fernandez JE, Deaglio S, Donati D, Beusan IS, Corno F, Aranega A, et al. Analysis of the distribution of human CD38 and of its ligand CD31 in normal tissues. J Biol Regul Homeost Agents 1998;12:81–91.
18. Su A, MacLeod WC. BioGPS. [Cited 2012 May 9]. Available from: http://biogps.org/gene/952/.
19. de Weers M, Tai YT, van der Veer MS, Bakker JM, Vink T, Jacobs DCH, et al. Daratumumab, a novel therapeutic human CD38 monoclonal antibody, induces killing of multiple myeloma and other hematological tumors. J Immunol 2011;186:1840–8.
20. Tesar M. Fully human antibody MOR202 against CD38 for the treatment of multiple myeloma and other blood-bourne malignancies. J Clin Oncol 2007;25:8106.
21. Vooijs WC, Schuurman HJ, Bast EJ, de Gast GC. Evaluation of CD38 as target for immunotherapy in multiple myeloma. Blood 1995;85: 2282–4.
22. Goldmacher VS, Bourret LA, Levine BA, Rasmussen RA, Pourshadi M, Lambert JM, et al. Anti-CD38-blocked ricin: an immunotoxin for the treatment of multiple myeloma. Blood 1994;84:3017–25.
23. Bolognesi A, Polito L, Farini V, Bortolotti M, Tazzari PL, Ratta M, et al. CD38 as a target of IB4 mAb carrying saporin-S6: design of an immunotoxin for ex vivo depletion of hematological CD38+ neoplasia. J Biol Regul Homeost Agents 2005;19:145–52.
24. Goldenberg DM, Chang CH, Sharkey RM, Rossi EA, Karacay H, McBride W, et al. Radioimmunotherapy: is avidin-biotin pretargeting the preferred choice among pretargeting methods? Eur J Nucl Med Mol Imaging 2003;30:777–80.
25. Forero A, Weiden PL, Vose JM, Knox SJ, LoBuglio AF, Hankins J, et al. A Phase I trial of a novel anti-CD20 fusion protein in pretargeting radioimmunotherapy for B cell non-Hodgkin's lymphoma. Blood 2004;104:227–36.

26. Axworthy DB, Fritzberg AR, Hylarides MD, Mallett RW, Theodore LJ, Gustavson LM, et al. Preclinical evaluation of an anti-tumor monoclonal antibody/streptavidin conjugate for pretargeted Y-90 radioimmunotherapy in a mouse xenograft model. J Immunother. 1994;16:158.
27. Press OW, Corcoran M, Subbiah K, Hamlin DK, Wilbur DS, Johnson T, et al. A comparative evaluation of conventional and pretargeted radioimmunotherapy of CD20-expressing Lymphoma Xenografts. Blood 2001;98:2535–43.
28. Graves SS, Dearstyne E, Lin Y, Zuo Y, Sanderson J, Schultz J, et al. Combination therapy with pretarget CC49 radioimmunotherapy and gemcitabine prolongs tumor doubling time in a Murine Xenograft model of colon cancer more effectively than either monotherapy. Clin Cancer Res 2003;9:3712–21.
29. Schultz J, Lin Y, Sanderson J, Zuo Y, Stone D, Mallett R, et al. A tetravalent single-chain antibody-streptavidin fusion protein for pretargeted lymphoma therapy. Cancer Res 2000;60:6663–9.
30. Mirzadeh S, Brechbiel MW, Atcher RW, Gansow OA. Radiometal labeling of immunoproteins: covalent linkage of 2-(4- isothiocyanatobenzyl)diethylenetriaminepentaacetic acid ligands to immunoglobulin. Bioconjugate Chem 1990;1:59–65.
31. Park SI, Shenoi J, Frayo SM, Hamlin DK, Lin Y, Wilbur DS, et al. Pretargeted radioimmunotherapy using genetically engineered antibody-streptavidin fusion proteins for treatment of non-hodgkin lymphoma. Clin Cancer Res 2011;17:7373–82.
32. Pressman D, Day ED, Blau M. The use of paired labeling in the determination of tumor-localizing antibodies. Cancer Res 1957;17: 845–50.
33. Fisher DR, Shen S, Meredith RF. MIRD dose estimate report no. 20: radiation absorbed-dose estimates for 111In- and 90Y-ibritumomab tiuxetan. J Nucl Med 2009;50:644–52.
34. Hui TE, Fisher DR, Kuhn JA, Williams LE, Nourigat C, Badger CC, et al. A mouse model for calculating cross-organ beta doses from yttrium-90- labeled immunoconjugates. Cancer 1994;73:951–7.
35. Beatty BG, Kuhn JA, Hui TE, Fisher DR, Williams LE, Beatty JD. Application of the cross-organ beta dose method for tissue dosimetry in tumor-bearing mice treated with a 90Y-labeled immunoconjugate. Cancer 1994;73:958–65.
36. Press OW, Shan D, Howell-Clark J, Eary J, Appelbaum FR, Matthews D, et al. Comparative metabolism and retention of iodine-125, yttrium-90, and indium-111 radioimmunoconjugates by cancer cells. Cancer Res 1996;56:2123–9.
37. Press OW, Howell-Clark J, Anderson S, Bernstein I. Retention of B-cell-specific monoclonal antibodies by human lymphoma cells. Blood 1994;83:1390–7.
38. Paganelli G, Grana C, Chinol M, Cremonesi M, De Cicco C, De Braud F, et al. Antibody-guided three-step therapy for high grade glioma with yttrium- 90 biotin. Eur J Nucl Med 1999;26:348–57.
39. DeNardo DG, Xiong CY, Shi XB, DeNardo GL, DeNardo SJ. Anti-HLA-DR/anti-DOTA diabody construction in a modular gene design platform: bispecific antibodies for pretargeted radioimmunotherapy. Cancer Biother Radiopharm 2001;16:525–35.
40. Leigh BR, Kurtts TA, Mack CF, Matzner MB, Shimm DS. Radiation therapy for the palliation of multiple myeloma. Int J Radiat Oncol Biol Phys 1993;25:801–4.
41. Bink K, Haralambieva E, Kremer M, Ott G, Beham-Schmid C, de Leval L, et al. Primary extramedullary plasmacytoma: similarities with and differences from multiple myeloma revealed by interphase cytogenetics. Haematologica 2008;93:623–6.
42. Berenson JR, Yellin O, Patel R, Duvivier H, Nassir Y, Mapes R, et al. A phase I study of samarium lexidronam/bortezomib combination therapy for the treatment of relapsed or refractory multiple myeloma. Clinical Cancer Res 2009;15:1069–75.
43. Green DJ, Pagel JM, Nemecek ER, Lin Y, Kenoyer A, Pantelias A, et al. Pretargeting CD45 enhances the selective delivery of radiation to hematolymphoid tissues in nonhuman primates. Blood. 2009;114: 1226–35.
44. Subbiah K, Hamlin DK, Pagel J, Wilbur DS, Meyer DL, Axworthy DB, et al. Comparative immunoscintigraphy, toxicity, and efficacy of conventional and pretargeted radioimmunotherapy in a CD20-expressing human lymphoma xenograft model. J Nucl Med 2003;44:437–45.
45. Pagel JM, Orgun N, Hamlin DK, Wilbur DS, Gooley TA, Gopal AK, et al. A comparative analysis of conventional and pretargeted radioimmunotherapy of B-cell lymphomas by targeting CD20, CD22, and HLA-DR singly and in combinations. Blood 2009;113:4903–13.
46. Ma D, McDevitt MR, Barendswaard E, Lai L, Curcio MJ, Pellegrini V, et al. Radioimmunotherapy for model B cell malignancies using 90Y-labeled anti-CD19 and anti-CD20 monoclonal antibodies. Leukemia 2002;16:60–6.
47. Tuscano JM, O'Donnell RT, Miers LA, Kroger LA, Kukis DL, Lamborn KR, et al. Anti-CD22 ligand-blocking antibody HB22.7 has independent lymphomacidal properties and augments the efficacy of 90Y-DOTA-peptide-Lym-1 in lymphoma xenografts. Blood 2003;101: 3641–7.
48. Sharkey RM, Karacay H, Litwin S, Rossi EA, McBride WJ, Chang CH, et al. Improved therapeutic results by pretargeted radioimmunotherapy of non-Hodgkin's lymphoma with a new recombinant, trivalent, anti-CD20, bispecific antibody. Cancer Res 2008;68:5282–90.
49. LeBlanc R, Catley LP, Hideshima T, Lentzsch S, Mitsiades CS, Mitsiades N, et al. Proteasome inhibitor PS-341 inhibits human myeloma cell growth in vivo and prolongs survival in a murine model. Cancer Res 2002;62:4996–5000.
50. Lentzsch S, LeBlanc R, Podar K, Davies F, Lin B, Hideshima T, et al. Immunomodulatory analogs of thalidomide inhibit growth of Hs Sultan cells and angiogenesis in vivo. Leukemia 2003;17:41–4.